Journal of Solid State Chemistry 182 (2009) 1424–1429

Contents lists available at ScienceDirect

Journal of Solid State Chemistry

journal homepage: www.elsevier.com/locate/jssc

Light induced magnetic properties of spiropyrane tris(oxalato)chromate (III) single crystals

R.B. Morgunov [a,*], F.B. Mushenok [a], S.M. Aldoshin [a], E.A. Yur'eva [a], G.V. Shilov [a], Y. Tanimoto [b]

[a] Institute of Problems of Chemical Physics RAS, Chernogolovka, Chernogolovka, Ak. Semenova, 1, Moscow Region 142432, Russian Federation
[b] Faculty of Pharmacy, Osaka Ohtani University, Nishikiorikita, Tondabayashi 584-8540, Japan

ARTICLE INFO

Article history:
Received 7 October 2008
Received in revised form
11 March 2009
Accepted 16 March 2009
Available online 26 March 2009

PACS:
75.50.Xx
72.80.Ga

Keywords:
Molecular magnets
Transition metal compounds
ESR
Zero-field splitting

ABSTRACT

The effect of UV light on Weiss temperature and ESR spectra in 1-isopropyl-3, 3, 5′, 6′-tetramethylspiro[indolin-2,2′-[2*H*]pyrano[3,2-*b*]pyridinium] tris(oxalato)chromate (III) ($Sp_3Cr(C_2O_4)_3$) has been found. Additional line has been observed in the ESR spectra of irradiated samples in "strong" magnetic fields of ~15 kOe. The analysis of angular dependences of the ESR spectra allowed a contribution of Cr^{3+} ions to magnetic properties of $Sp_3Cr(C_2O_4)_3$ to be determined. The zero-field splitting parameters $D = 0.619\,cm^{-1}$, $E = 0.024\,cm^{-1}$ were derived from the experimental data. The parameters were typical for Cr^{3+} in the chromium oxalate. Weiss temperature changed sign from 25 to −25 K under UV irradiation. The value of Weiss temperature and its changing cannot be explained by exchange interaction, dipole–dipole interaction or the effect of crystal field. The existence of Weiss temperature is explained by the changes in amount and spin of paramagnetic particles. The change is due to thermoactivated redistribution of electrons between chromium ions and spiropyrane molecules. Light-induced transfer of electrons is also explaining the change in sign of Weiss temperature under UV irradiation.

1. Introduction

One of the urgent tasks of state-of-the-art crystal-chemical engineering is preparation of materials whose magnetic properties can be governed with light [1–6]. One of ideas of realizing such structures consists in combining photochromic molecules (spiropyranes, spirooxazines) and magnetic complexes of transition metals in the same crystal lattice. One could expect that changes in the structure of spiran molecules under light would provide changes in crystal fields and exchange interactions in magnetic sublattices [1]. The first efforts to design such materials demonstrated principally possible observation of photomagnetic effects in them [2]. However, mechanisms of structural changes under light were not clarified. In particular, interrelation between crystal structure and magnetic properties of the compounds were not established in first experiments. The only effect observed was the low-temperature change in hysteresis loop shape under light [2]. We studied $Sp_3Cr(C_2O_4)_3$ recently synthesized, SP = 1-isopropyl-3, 3, 5′, 6′-tetramethylspiro[indolin-2,2′-[2*H*]pyrano[3,2-*b*]pyridinium] cation [7]. The goals of the study were to separate contributions of different subsystems to magnetic properties of $Sp_3Cr(C_2O_4)_3$, estimate the splitting parameters of spin levels in crystal field, find the effect of UV light on magnetic properties and establish interrelation between crystal structure and magnetic properties.

2. Experimental

By mixing 0.6 mmol of SPCl and 0.2 mmol of $K_3Cr(C_2O_4)*3H_2O$, dissolved separately in a minimum of water, the $Sp_3Cr(C_2O_4)*4H_2O$ was obtained as a pale green powder [2]. Optically transparent single crystals were grown by crystallization from aqueous ethanol. The X-ray analysis showed [7] the crystal structure to be of trigonal syngony, space group $P(-3)$, $Z = 2$. The crystal structure involves three SP^+ cations per one $[Cr(C_2O_4)_3]^{3-}$ anion. One unit cell involves two such neutral units linked by the inversion center. Cr atoms are located in $Cr(C_2O_4)_3$ in octahedra on the 3-fold axes. Therefore, only one oxalate ligand is chelately coordinated of chromium ion and is structurally independent. Fig. 1 shows the fragment of crystal structure of $Sp_3Cr(C_2O_4)_3$. Full crystallographic information can be found in [7].

Photochromic reaction in spyropiran based compounds proceeds by rupture of C–O bond and further isomerization of molecules (inset on Fig. 2). Open form of spiropyran is amount of closed form transformation under UV irradiation [7]. Absorption bands at the 574 and 603 nm wavelength of the open form appear

* Corresponding author. Fax: +8 49652 49676.
E-mail address: morgunov2005@yandex.ru (R.B. Morgunov).

0022-4596/$ - see front matter © 2009 Elsevier Inc. All rights reserved.
doi:10.1016/j.jssc.2009.03.011

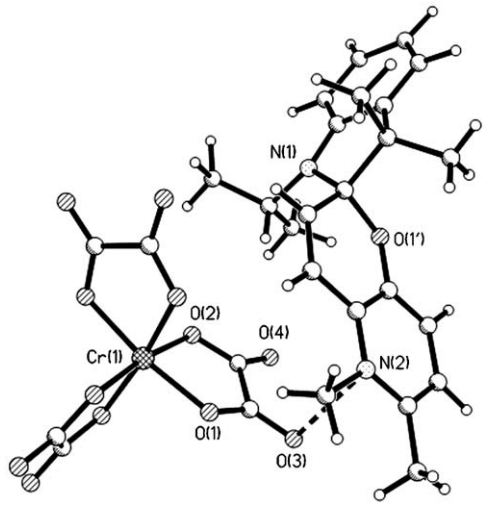

Fig. 1. Fragment of crystal structure of $SP_3Cr(C_2O_4)_3$. Contact of 3.05 Å between oxalate oxygen atom and spiropyrane nitrogen atom is shown by dashed lines.

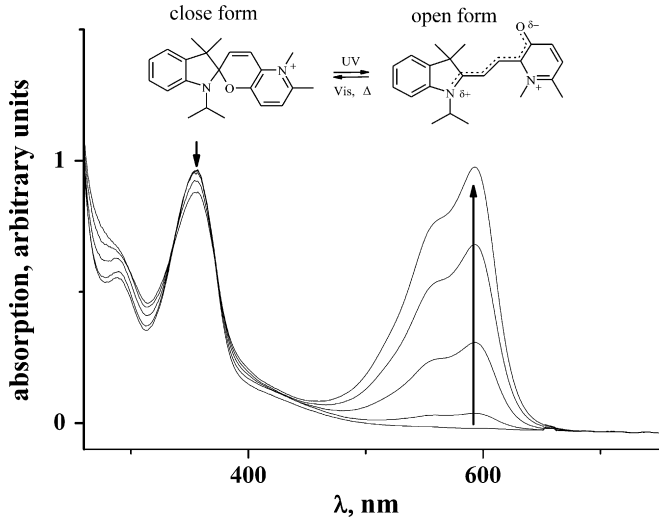

Fig. 2. The absorption spectra of $SP_3Cr(C_2O_4)_3$ crystal before and after UV irradiation with $\lambda = 355$ nm. Inset shows opening of spyropiran molecule under UV irradiation.

under UV irradiation $\lambda = 355$ nm (Fig. 2). After irradiation of visible light ($\lambda = 530$ nm) this band is disappear. Another kind of light excitation corresponded by absorbtion line lying at 350 nm. This line correspond band gap transition.

The dependences of DC (direct current) magnetic moment M for the $Sp_3Cr(C_2O_4)_3$ powder in the field of $H = 1000$ Oe at $T = 2$–300 K and $H = 0$–50 kOe at $T = 2$ K were measured using a MPMS 5XL SQUID magnetometer (Quantum design). The irradiation by UV light was performed for 2 h at room temperature outside a SQUID magnetometer by an xenon lamp using the filter transmitting in the range $\lambda = 250$–450 nm. To provide the access of light to all microcrystals of the powder, the sample was stirred upon irradiation.

High-frequency spin dynamics and separation of contributions from different type particles to magnetic susceptibility χ of the samples were studied using a Bruker EMX ESR spectrometer operating in the X-band ($\nu = 9.432$ GHz) equipped with a H_{102} type rectangular resonator with 100 KHz modulation frequency and 0–16 kOe magnetic field scan range. Frequency was controlled by frequency meter. Casual variations of the frequency were possible in a fifth digit. These variations were smaller than accuracy of g measurements. Single crystal $CuSO_4 * 5H_2O$ was used as a reference sample. Temperature was varied from 6 up to 280 K within 1 K accuracy in a ESR900 Oxford Instruments cryostat. While studying magnetic properties of $Sp_3Cr(C_2O_4)_3$ single crystals with the ESR spectrometer, we obtained the dependences of the first derivative of microwave absorption dI/dH on crystal orientation at constant $T = 295$ K (before and after irradiation) and the temperature dependence of the first derivative of microwave absorption at fixed crystal position (before irradiation). The crystal was rotated in the ac plane. Additional measurements were performed in $\mathbf{H}||b$ orientation.

3. Results

Magnetic moment of powder-like sample has been measured with a SQUID-magnetometer. Temperature dependencies of reciprocal magnetic moment of the sample are shown in Fig. 3 before and after UV irradiation. Linear extrapolation of high-temperature portions of these curves to zero value of $1/M$ results in Weiss temperatures $T_{0\ \mathrm{dark}} = 25$ K before and $T_{0\ \mathrm{light}} = -25$ K after irradiation. Thus, UV irradiation induces alteration of Weiss constant sign.

The ESR spectra measured on single crystals were analyzed in the second series of experiments. The ESR spectra of non-irradiated crystals are to be described first. The temperature dependence of the first derivative of microwave absorption was measured from 6 up to 280 K at an angle Θ between the direction of static magnetic field H and the c-axis of the crystal equal to 10°, and $\mathbf{H} \perp b$ (Fig. 4). At such crystal orientation, the ESR spectrum shows the maximal (8) number of lines and, hence, most detailed information on transitions between spin levels.

Fig. 5 shows the dependence of resonance fields of the ESR lines on angle Θ between the c axis and the direction of external field H at $T = 295$ K. The angle between the crystallographic b axis and the direction of external field $\mathbf{H}$ was retained constant and equal to 90°. From 3 to 8 resonance lines were observed in the spectrum depending on crystal orientation. Lines 1–3 merged into one line with angle Θ increasing from 0° to 90°, and corresponding resonance frequency decreased. Lines 4 and 5 were observed only at angles Θ ranging from 0° to 35°. Moreover, line 5 split into two components at $\Theta = 30$–35°. The values of resonance fields for lines 6–8 increased with angle Θ and at Θ growing from 20° up to 160° the lines were not observed.

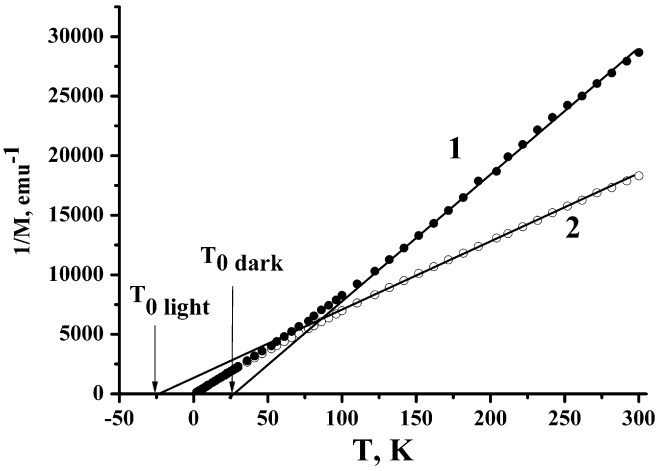

Fig. 3. Temperature dependences of reciprocal molar magnetic moment of the sample at $T = 2$ K: (1) before irradiation, and (2) after UV irradiation.

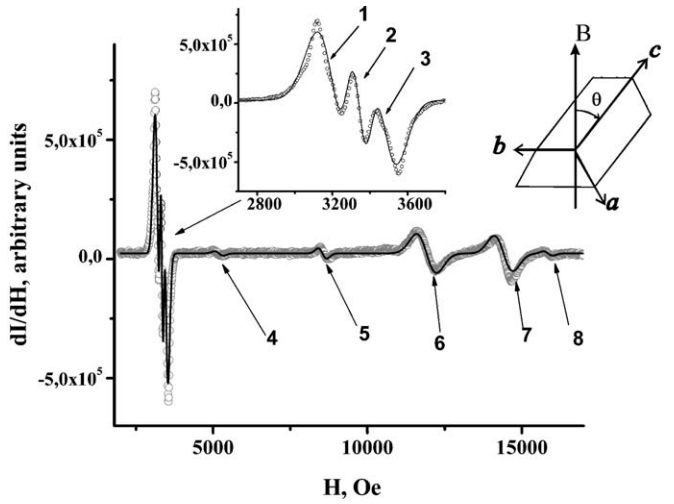

Fig. 4. ESR spectrum of $SP_3Cr(C_2O_4)_3$ single crystal at $T = 15$ K, $\Theta = 10^\circ$. Experimental data are shown by points, approximation with eight Gaussian lines is shown by full line. Insets show crystal orientation in applied magnetic field and the fragment of the ESR spectrum near g-factor of free electron.

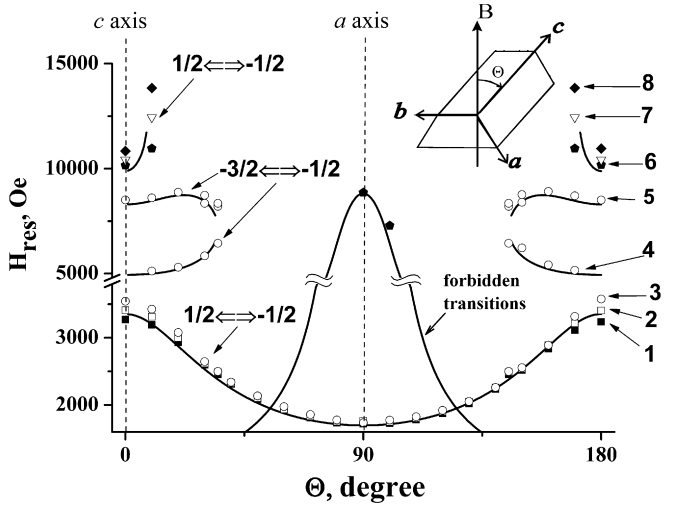

Fig. 5. Dependence of ESR resonance fields on angle Θ between field direction and crystal c-axis in $SP_3Cr(C_2O_4)_3$ single crystals; static magnetic field is perpendicular to crystal b-axis ($B \perp b$), $T = 295$ K. Approximation with Eqs. (2) and (3) are shown by solid lines (see text). Inset shows crystal orientation relative to magnetic field B and angle Θ.

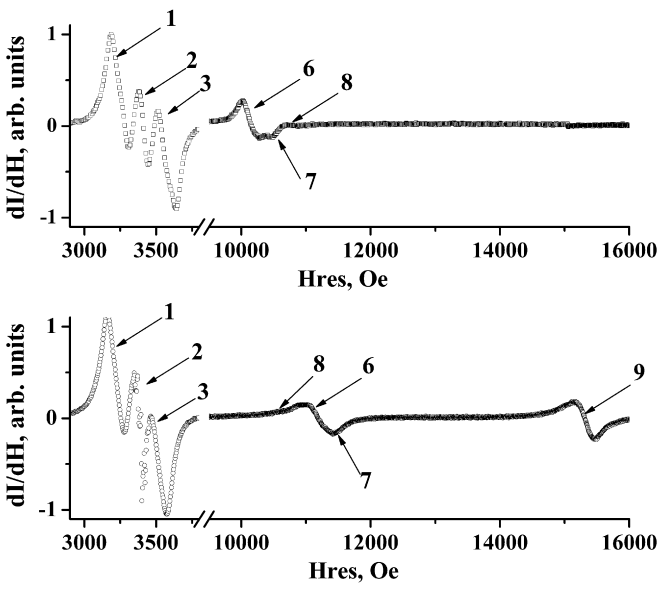

Fig. 6. ESR spectrum before (above) and after (below) irradiation. Angle Θ between static magnetic field direction and crystal c-axis is 0°.

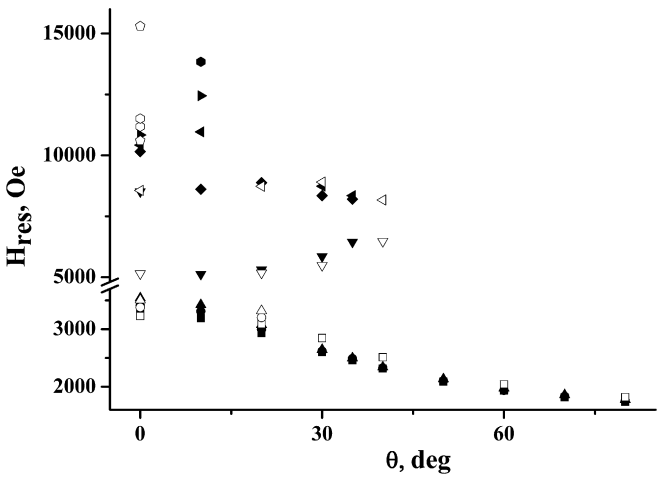

Fig. 7. Dependence of ESR resonance fields on angle Θ between field direction and crystal c-axis in $SP_3Cr(C_2O_4)_3$ single crystals before (black symbols) and after (white symbols) irradiation. Static magnetic field is perpendicular to the crystal b axis ($B \perp b$), $T = 295$ K.

To determine resonance spin transition parameters (resonance fields and linewidths), we approximated all the ESR spectra with the Gaussian-shaped lines, which described the spectrum better than the Lorentzian ones. Thus, non-uniform broadening took place probably as a result of crystal inhomogeneity.

Resonance field is almost temperature independent for all spectral lines in the 280–30 K range and at $T < 30$ K only we observed weak changes in effective g-factors of all lines. Temperature independence of H_{res} indicates the absence of phase transitions which can affect Weiss constant. The $CuSO_4 * 5H_2O$ sample was used as a reference one. Strong spectrum of the reference sample covered $(-1/2)$–$(+1/2)$ transition. For that reason intensity of other transitions were calibrated and recalculated for $(-1/2)$–$(1/2)$ transition. Calibration was compared with effective magnetic moment, received by SQUID magnetometer. At room temperature this calibration indicate combined contribution of $S = 3/2$ and low-spin $S = 1$ particles in the "dark" crystals.

When angular and temperature dependences for the ESR spectrum were measured, the $Sp_3Cr(C_2O_4)_3$ single crystal was irradiated by a UV xenon lamp for 2 h. Then the angular dependence of ESR was measured at Θ ranging from 0° to 90°. Fig. 6 shows for comparison two ESR spectra before and after irradiation, and Fig. 7 shows the angular dependence of resonance fields of the ESR spectrum before and after irradiation. Since the irradiated crystal repeatedly placed in a ESR resonator inevitably has another orientation differing by ~10° (experimental error), line positions depend on angle Θ. A criterion for correct comparison of the spectra before and after irradiation was a coincidence of positions of resonance fields for lines 1–3 in the spectra of irradiated and non-irradiated crystals. Such criterion allowed sample orientation in a spectrometer to be calculated with high accuracy (~0.1°) and possible changes in the spectra initiated by UV light to be proved. It was found from the analysis of the angular dependences for lines 1–3 that the position of the

crystal irradiated by UV light corresponded to the angle $\Theta = 3.8^\circ$. With high reliability lines 4 and 5 (not shown in Fig. 6) occupied the same positions that before irradiation due to weak angular dependence of the lines in the experimental angle range. The shift of lines 6–8 to higher fields was calculated for $\Theta = 3.8^\circ$ and coincided with their new positions when the irradiated sample was placed in a resonator. Therefore, the positions of the lines remained unchanged. Additional line 9 observed in the ESR spectrum of the irradiated crystal at resonance field $H_{res} = 15\,300$ Oe was not observed in the starting non-irradiated sample at neither angle value in the 0–180° range. A conclusion can be drawn on that the line is a new one, i.e. appeared as a result of UV irradiation.

4. Discussion

The Cr^{3+} cation is in octahedral ligand field in the oxalate molecule. Thus, the spin Hamiltonian for the Cr^{3+} cation in the ground state $^4A_2$ is [8]

$$\hat{H} = \mu_b HgS + D[S_z^2 - S(S+1)/3] + E(S_x^2 - S_y^2) \quad (1)$$

$S = \frac{3}{2}$ is spin of the Cr^{3+} cation; μ_B is Bohr magneton; g is Lande splitting factor; D and E are zero-field splitting parameters. As a result, ligand field splits four spin levels into two doublets (Fig. 8). The value of splitting between spin levels is $2(D^2+3E^2)^{1/2}$.

When magnetic field is applied parallel to the z axis, the transition energy can be written as follows:

$$\Delta E_z(\tfrac{1}{2} - (-\tfrac{1}{2})) = g_{zz}\mu_B H - [(D + g_{zz}\mu_B H)^2 + 3E^2]^{1/2} + [(D - g_{zz}\mu_B H)^2 + 3E^2]^{1/2} \quad (2)$$

$$\Delta E_z(-\tfrac{3}{2} - (-\tfrac{1}{2})) = 2[(D - g_{zz}\mu_B H)^2 + 3E^2]^{1/2} \quad (3)$$

It derives from the equations set that lines 1–3 (Fig. 5) correspond to the (−1/2)–(1/2) transition, lines 4 and 5 correspond to the (−3/2)–(−1/2) transition in weak and strong fields, and lines 6–8 correspond to the (−1/2)–(1/2) transition in strong magnetic field. The splitting into two lines is observed for line 5 at angles $\Theta = 30$–35° between magnetic field direction and the c axis. Single experimental points at angles of 90–100° at $H_{res} = 7$–9 kOe correspond to the (3/2)–(1/2) transition forbidden at small angles Θ.

Three resonant fields at $\Theta = 0^\circ$ correspond spin transitions described above (Fig. 5). Eqs. (2) and (3) allow us to find three independent variables g_z, D, E. These values served us as initial

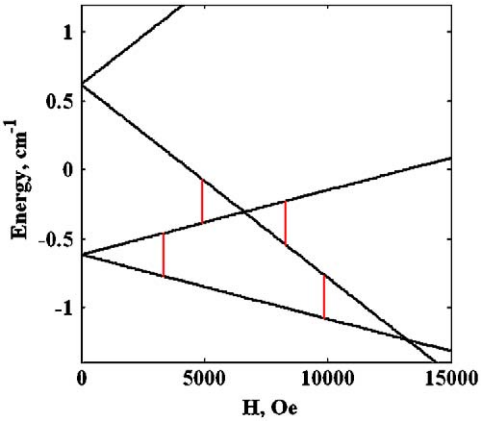

Fig. 8. Energies of spin levels of Cr^{3+} ions ($E \ll D$) and spin transitions (vertical red line) simulated by spin-Hamiltonian discussed in the text. (For interpretation of the references to color in this figure legend, the reader is referred to the web version of this article.)

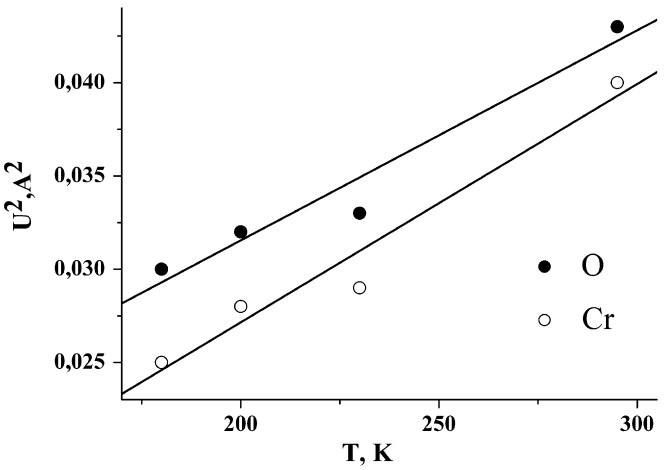

Fig. 9. Temperature dependence of squared amplitude of thermal vibrations U^2 for: atom Cr1 and one of oxygen atoms O1. Linear extrapolation is shown by solid line.

parameters for approximation of angular dependence at all orientation, including **H**||*b*. This approximation performed by Matlab software gives g_{xx} and g_{yy} parameters. Theoretical angular dependence (solid line in Fig. 5) was generated EasySpin software [9]. Finally, we obtained parameters $g_{zz} = g_{xx} = g_{yy} = 1.956$, $D = 0.619\,cm^{-1}$, and $E = 0.024\,cm^{-1}$.

These crystal filed splitting parameters are in good agreement with the data obtained for $Cr(C_2O_4)_3$ in $NaMgAl(C_2O_4)_3 * 9H_2O$ [10] and $K_3Al(C_2O_4) * 3H_2O$ [11] single crystals. Therefore, a conclusion can be drawn on that lines 1–8 correspond to electron spin resonance on Cr^{3+} ions. The presence of three resonance lines 1–3, which correspond to the same (−1/2)–(1/2) transition can be due to distorted octahedral environment of Cr atoms.

This assumption was proved by X-ray experiments. The calculations showed that both independent Cr–O bonds (Fig. 1) are similar within experimental error. It should be noted that the refinement of the structure using non-centrosymmetrical group *P*3 yielded equally long Cr–O bonds in both independent $[Cr(C_2O_4)_3]^{3-}$ anions of different chirality. It is known that crystal structure determined from X-ray analysis is averaged in space and time. Thus, small structural differences related to statistical displacement of atoms from average positions cannot be determined directly in some cases, especially when such displacements are close to the amplitude of thermal vibrations of atoms. To reveal possible presence of these permanent small displacements of atoms in crystal structure we performed X-ray analysis of a crystal of the compound at different temperatures. From the experimental data, amplitudes of thermal vibrations of atoms were calculated and the plots of temperature dependences of squared amplitude of thermal vibrations were made (Fig. 9). It is known that this dependence is linear in harmonic approximation in the classical range and squared amplitude of thermal vibrations must tend to zero at temperature extrapolation to zero. However, if atomic position is average statistical of two and more close ones, a temperature independent additional value appears in atomic parameters. Thus, if one linearly extrapolates the plot of temperature dependence of squared amplitude of atomic thermal vibrations, a segment will be cut off on the *Y*-axis proportional to the squared distance between disordered atomic positions. Particularly, there are two close positions for atom in the structure. This value is $\mu(1-\mu)\Delta^2$, where μ and $(1-\mu)$ are probabilities of atoms location in these positions and Δ is distance between these positions. Fig. 9 shows the temperature dependences of squared amplitude of thermal vibrations U^2 for

chromium atom Cr1 and one of chromium coordinating oxygen atom O1.

It was found for Cr atom that squared amplitude of thermal vibrations U^2 tends to zero with temperature T tending (Fig. 9). However, components of ellipsoids of thermal vibrations were found for oxygen atoms which involved noticeable temperature independent additives. For O(1) it was $\sim 0.010\,\text{Å}^2$ that is greater than experimental error (Fig. 9). This additive indicates the Cr–O bond to be average statistical in two bonds at the least. Thus, real octahedron geometry is slightly different from average one.

It is of importance that the greatest statistical additive magnitude to thermal parameter is observed for oxygen atom O(1) probably due to structural features. The oxalate ion is −2 charged. The charge can be located on atoms O(1) and O(2), and O(2) and O(3) as well. The latter suggestion is based on the fact that cation positive charge is nitrogen atom N(2), and a contact is observed between this atom and oxygen atom O(3) in the crystal structure (Fig. 1). Negative charge redistribution between atoms O(2) and O(3) provides two types positions for atom O(1) in the structure at the least, which can result in the appearance of temperature independent additional value in its thermal parameters. Thus, chromium atom is in distorted octahedral environment rather than in regular one to provide energy level splitting. Distorted octahedral environment can provide the presence of several closely positioned lines of the ESR spectra attributed to the same transition. Thus, X-ray analysis showed the presence of three non-equivalent positions for $Cr(C_2O_4)_3$ responsible for the ESR lines splitting.

Exchange interaction, dipole–dipole magnetic interaction, splitting of spin levels by crystal field as well as thermoactivated electron processes is able to contribute to Weiss temperature. Estimations of each mentioned factors presented below.

Molar magnetic susceptibility of crystals, containing paramagnetic ions Cr^{3+} in axial ligand field can be described by the following equation containing splitting parameter D [12]:

$$\chi_{||} = \frac{N_A g_{||}^2 \mu_B^2}{4kT}\left[\frac{1+9\,\exp(-2D/kT)}{1+\exp(-2D/kT)}\right] \quad (4)$$

$$\chi_{\perp} = (N_A g_{\perp}^2 \mu_B^2/4\,\text{kT})[1+\exp(-2D/kT)]^{-1} + (3N_A g_{\perp}^2 \mu_B^2/4D)\tanh(D/kT) \quad (5)$$

$\chi_{||}$, $\chi\perp$—are "in-plane" and "out-of-plane" magnetic susceptibilities, respectively; N_A—is Avogadro constant; $g_{||}$, $g\perp$—are "in-plane" and "out-of-plane" g-factors, respectively; μ_B—is Bohr magneton; and k—Boltzmann constant.

Magnetic susceptibility of a powder sample was calculated from

$$\chi = \frac{2\chi_{||} + \chi_{\perp}}{3} \quad (6)$$

Using Eqs. (4)–(6) we calculated contribution of the crystal field to Weiss temperature 0.6 K. This value is negligibly small in comparison with the experimentally obtained 25 K. Thus, the value of Weiss constants and its changes under irradiation cannot be explained by crystal field splitting.

Magnetic dipole–dipole interaction between Cr^{3+} spin moments and its contribution to the Weiss constant was estimated from formula [13]:

$$\frac{E_{dip}}{k} = \frac{(g\mu_b S)^2}{kV}$$

V is crystal cell volume $2.23\times10^{-27}\,\text{m}^3$. This contribution of 2.5 mK is also negligibly small and cannot be used to describe the observed photomagnetic effect.

Long distance between Cr spins ~12.8 A prevents any direct exchange interaction. Indirect exchange interaction is also impossible in the studied crystals, because of the absence of covalent chemical bonds between molecules in crystal lattice. Thus, exchange interaction, dipole–dipole magnetic interaction and spin levels splitting by crystal field could not be used to describe the Weiss constant value and its changes under irradiation. Possible reason of Weiss temperature existing is thermoactivated transition of electrons between impurity levels in band gap (Fig. 10). Impurity levels originate from crystal lattice defects resulted from ionized molecules of spiropyrane and Cr^{4+} ions ($3d^2$, $S=1$) generated by UV irradiation. The Cr^{4+} ions can be reduced to Cr^{3+} ions by electrons capture [14]. Thus, crystal lattice includes both Cr^{3+} ($S=\frac{3}{2}$) and Cr^{4+} ($S=1$) ions. If impurity levels are localized near the top of the valence band ($\sim kT$), recombination of Cr^{4+} into Cr^{3+} and ionization of Cr^{3+} into Cr^{4+} will take place due to thermal fluctuation, and population of impurity levels will be temperature dependent. In this wise, the changes in temperature produce the changes in high-spin (Cr^{3+}, $S=\frac{3}{2}$) to low-spin (Cr^{4+}, $S=1$) ion concentration ratio. Since amount of paramagnetic particles with equal spin depends on temperature, magnetic moment is also temperature dependent that results in deviation from the Curie law and non-zero Weiss temperature. The thermoactivated transitions of electrons also explain alteration of sign of Weiss temperature from $T_{0\ \text{dark}} = 25$ K to $T_{0\ \text{light}} = -25$ K. UV irradiation changes populations of impurity levels and modifies distribution of high- and low-spin chromium ions. Thus, UV irradiation changes the temperature dependence of magnetic moment and Weiss temperature.

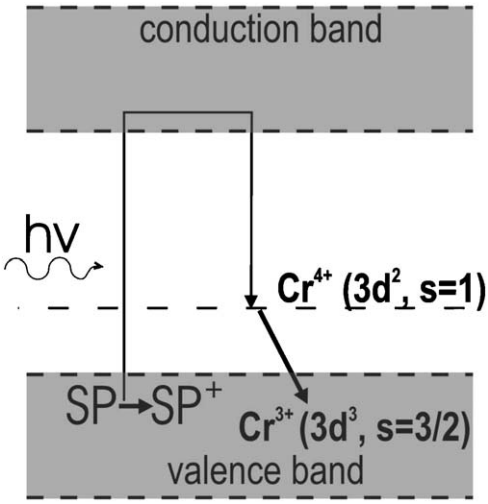

Fig. 10. Possible position of energy levels Cr^{3+} H Cr^{4+} ions in band model of crystal.

There are two possible explanations of origin of additional line 9 in ESR spectrum (Fig. 6). One explanation is creation of paramagnetic centers on spiropyran molecules. Earlier, ESR signal at $g=4$ was observed in Langmuir–Blodgett films containing open form of spiropyran [15]. The ESR signal was explained by triplet states of open spiropyran molecules. Spiropyran [16] and some organic molecules [17–19] show low-lying triplet excited states. Such thermal populated triplet states show paramagnetic properties. The temperature increase leads to growing number of triplet molecules and increase of ESR signals. Therefore, line 9 may corresponds to spin resonance on triplet molecules of spiropyran. Another explanation is existence of Cr^{4+} ions. It is well known that crystal field parameters for Cr^{4+} ions are stronger than ones for Cr^{3+} ions [8,14]. Since the additional ESR line 9 is observed in strong (~15 kOe) magnetic field, it may correspond to Cr^{4+} resonance.

5. Conclusion

The effect of UV light on Weiss temperature and the ESR spectra of the $Sp_3Cr(C_2O_4)_3$ crystals was found. The analysis of experimental data shows that additionally to the Cr^{3+} ion expected in the crystal structure, additional paramagnetic particles are present in the irradiated sample. The origin of high value of Weiss temperature is a deviation of the temperature dependence of magnetic moment from the Curie law. Its deviation is caused by thermal induced transitions of electrons between Cr^{3+} and Cr^{4+} ions and spiropyrane molecules. The UV irradiation of the sample stimulates the redistribution of electrons between impurity levels of defects and the valence band, and increases concentration of high-spin Cr^{3+} ions. Therefore, a ratio of Cr^{3+} to Cr^{4+} for irradiated samples is different from a Cr^{3+}/Cr^{4+} ratio the non-irradiated sample. Thus, the values of Weiss temperature for irradiated and non-irradiated sample are different. This phenomenon found broadens the limits of photomagnetic effects known now.

References

[1] R. Clément, S. Decurtins, M. Gruselle, C. Train, Monatsh. Chem. 134 (2003) 117.
[2] S. Bénard, E. Riviere, P. Yu, K. Nakatani, J.F. Delouis, Chem. Mater. 13 (2001) 159.
[3] S.M. Aldoshin, N.A. Sanina, V.I. Minkin, N.A. Voloshin, V.N. Ikorskii, V.I. Ovcharenko, V.A. Smirnov, N.K. Nagaeva, J. Mol. Struct. 826 (2007) 69.
[4] S.M. Aldoshin, N.A. Sanina, V.A. Nadtochenko, E.A. Yur'eva, V.I. Minkin, N.A. Voloshin, V.N. Ikorskiy, V.I. Ovcharenko, Russ. Chem. Bull. 56 (2007) 1095.
[5] S.M. Aldoshin, J. Photochem. Photobiol. A Chem. 200 (2008) 19.
[6] S.M. Aldoshin, L.A. Nikonova, V.A. Smirnov, G.V. Shilov, N.K. Nagaeva, Izv. Khim. 2050 (2005) 9 (in Russian).
[7] S.M. Aldoshin, E.A. Yur'eva, G.V. Shilov, L.A. Nikonova, V.A. Nadtochenko, E.V. Kurganova, R.B. Morgunov, Russ. Chem. Bull. 57 (2008).
[8] A. Carrington, A.D. McLachlan, Introduction to Magnetic Resonance With Application to Chemistry and Chemical Physics, Harper & Row, New York, Evaston, London, 1967.
[9] S. Stoil, A. Scheiger, J. Magn. Reson. 178 (2006) 42.
[10] R.A. Bernheim, E.F. Reichenbecher, J. Chem. Phys. 51 (1969) 997.
[11] D.C. Doetschman, J. Chem. Phys. 60 (1974) 2647.
[12] R.D. Chirico, R.L. Carlin, Inorg. Chem. 19 (1980) 3031.
[13] E.M. Chudnovsky, D.A. Garanin, Phys. Rev. Lett. 89 (2002), 157201-1.
[14] R.H. Hoskins, B.H. Soffer, Phys. Rev. 133 (1964) A490.
[15] W.-F. Zhang, Y.-B. Huang, Z.-Q. Zhu, J. Mater. Sci. Lett. 19 (2000) 805–807.
[16] R.B. Morgunov, F.B. Mushenok, S.M. Aldoshin, N.A. Sanina, E.A. Yur'eva, G.V. Shilov, V.V. Tkachev, New J. Chem. (2009), doi:10.1039/b822567b.
[17] Y. Morita, T. Aoki, K. Fukui, S. Nakazawa, K. Tamaki, S. Suzuki, A. Fuyuhiro, K. Yamamoto, K. Sato, D. Shiomi, A. Naito, T. Takui, K. Nakasuji, Angew. Chem. Int. Ed. 41 (2002) 1793.
[18] S. Nelsen, R. Ismagilov, Y. Teki, J. Am. Chem. Soc. 120 (1998) 2200.
[19] L. Xu, T. Sugiyama, H. Huang, Z. Song, J. Meng, T. Matsuura, Chem. Commun. 20 (2002) 2328.